

Compact stellarator-tokamak hybrid

S. A. Henneberg * and G. G. Plunk 

Max-Planck-Institut für Plasmaphysik, Wendelsteinstr. 1, 17489 Greifswald, Germany



(Received 12 January 2024; accepted 6 May 2024; published 4 June 2024)

Tokamaks and stellarators are the leading two magnetic confinement devices for producing fusion energy, begging the question of whether the strengths of the two could be merged into a single concept. To meet this challenge, we propose a first-of-its kind optimized stellarator-tokamak hybrid. Compared to a typical tokamak coil set, only a single simple type of stellarator coil has to be added which leads to a compact, volume- and transport-preserving magnetic field, with an added rotational transform that reaches levels thought to enhance stability.

DOI: [10.1103/PhysRevResearch.6.L022052](https://doi.org/10.1103/PhysRevResearch.6.L022052)

Tokamaks and stellarators have comparative weaknesses: Stellarators are often criticized for the relatively small plasma volume they achieve, and for their complicated electromagnetic coils, both numerous in type and difficult to build. On the other hand, tokamaks rely on plasma currents to generate the magnetic field, which can generate detrimental instabilities and which impedes a desired steady-state operation.

The idea of a stellarator-tokamak hybrid is simple and compelling: to combine the strengths of the two concepts into a single device. Ideally, it would offer large plasma volume (compactness), easily built coils, and simple and inherently steady-state operation. However, this has proved an elusive combination to realize.

Several stellarator-tokamak hybrid designs have been proposed in the past, such as the spherical stellarator concept [1,2] or the tokastar [3]. Hybrid machines like W7-A [4,5] and the Compact Toroidal Hybrid (CTH) device [6,7] have even been built and operated, yielding valuable insight into how the three-dimensional shaping of tokamaks can enhance stability. However, none of these hybrids have persevered transport properties, as stellarators have, by default, higher so-called neoclassical transport, and only carefully tailored stellarators perform as well as tokamaks in this regard [8].

Any hybrid device that could be considered as a reasonable basis for fusion energy must therefore be optimized for neoclassical transport. This suggests that the optimized class most closely related to tokamaks, so-called quasiaxisymmetric (QA) stellarators [9,10], must be considered. For these stellarators, the magnetic field strength possesses a hidden

symmetry that is revealed upon transformation to special (“Boozer”) coordinates [11].

QA stellarators are thus the natural choice for designing a hybrid, but existing designs possess a highly twisted shape that departs strongly from the simple toroidal symmetry of a tokamak. This allows such devices to generate significant rotation of the magnetic field lines, imparting confinement and the passive stability that characterizes stellarators. However, a quick survey of previous QA designs, for instance Refs. [8,9,12–14], reveals a downside of this strong shaping, namely that the axisymmetric volume contained within the stellarator coils is drastically smaller than that available for stellarator operation. This means the tokamak part in such a flexible hybrid would have an aspect ratio of above 5. A large portion of the volume of the device, one of the main contributors to the cost, would therefore be wasted. It is hard to conceive of a tokamaklike hybrid device based on such designs.

Instead, we devise a hybrid concept, shown in Fig. 1, based on a class of QA solutions found as perturbations of tokamak equilibria [15,16], which achieve significant rotational transform from nonaxisymmetric shaping without significantly disturbing the overall plasma volume. The rotational transform, measuring the number of poloidal turns a field line makes per toroidal turn [10], is known to be critical to stability and confinement. These special perturbed tokamak solutions are found by venturing into an unfamiliar area of design space (lower aspect ratio and/or higher field periods) that so far has seemed inaccessible to QA stellarators [17]. In this limit, the external rotational transform is intuitively generated by localized stellarator shaping on the inboard of the torus, in the form of a tightly grooved pattern in the magnetic surfaces; see Fig. 4(b). This odd arrangement seems to be the key to realizing a tokamaklike equilibrium with the character (e.g., external rotational transform) of a stellarator, and is the basis of our idea for a tokamak-stellarator hybrid.

The perturbed axisymmetric equilibrium, which we investigate in this paper, has a field period number of 4, meaning that it consists of four identical torus segments, and it has a net toroidal plasma current I_{tor} of ≈ 574 kA. The original tokamak

*Sophia.henneberg@ipp.mpg.de

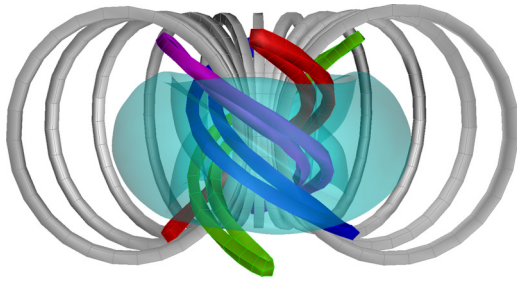


FIG. 1. The plasma boundary (cyan) encompassing four identical QA (“banana”) coils (red, green, blue, and purple) all contained within toroidal field coils (gray; half of them shown).

has a flat rotational transform profile of around 0.43, while the rotational transform of the original perturbed axisymmetric equilibrium ranges from 0.43 at the axis and increases to 0.56 at the plasma boundary, Fig. 2. The pressure and current density profiles are the ones used in Ref. [16] and are shown in Fig. 3 for convenience.

For the coils presented in this paper, we performed the second stage of the traditional two-stage approach [18]. This means that we optimized the coil geometry such that they can reproduce the plasma boundary found from the analytic theory by minimizing the normal components of the magnetic field on the fixed plasma boundary given by the theory. For this approach the profiles within the plasma are also fixed. Note that we did not optimize the plasma boundary any further, though it should certainly be possible to improve upon the perturbative near-axisymmetric solution. We will leave this task for future work.

For the coil optimization, we use the coil optimization features of the optimization framework `simsopt` [19,20]. We target, as typical in the two-stage approach, the quadratic-flux error functional

$$\varphi_2 = \frac{1}{2} \int |B_{E,n} - D_n|^2 ds, \quad (1)$$

where $\int ds$ is a surface integral over the plasma boundary, and $B_{E,n}$ is the normal component of the external magnetic field \mathbf{B}_E (produced by the coils) with respect to the plasma

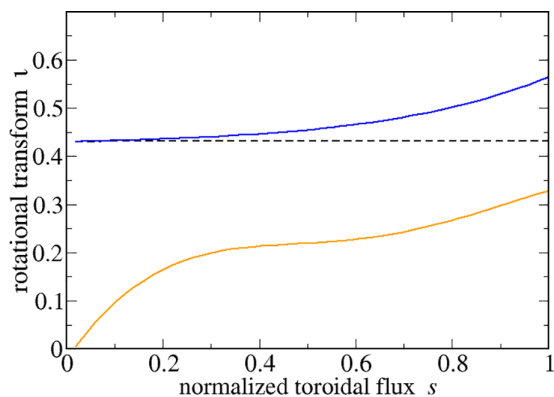


FIG. 2. Rotational transform ι versus normalized flux s ; The unperturbed, targeted case is in dashed black, the perturbed, targeted case is in solid blue, the rotational transform with altered profiles [14] (see Fig. 3) in solid orange.

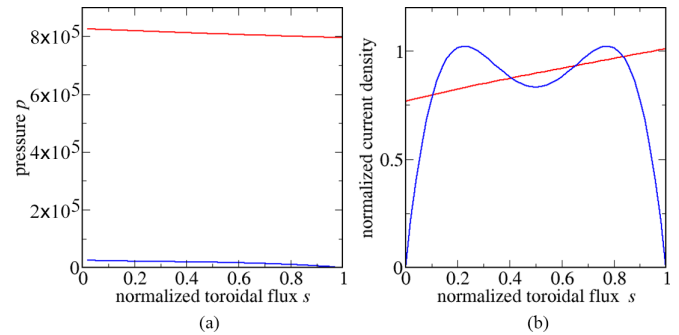


FIG. 3. The plasma profiles used in the analytic work and the evaluation of the coils based on Ref. [16] in red as well as the altered plasma profiles based on Ref. [14] in blue. Left: pressure profiles vs normalized toroidal flux. Right: normalized current density vs normalized toroidal flux.

boundary. D_n is the targeted normal component of the external magnetic field. In vacuum $D_n = 0$, since the plasma boundary is a flux surface. When investigating finite-beta plasmas, as done here, one has to determine the magnetic field produced by plasma currents to be able to calculate D_n . We used the so-called virtual casing method [21] for this purpose. The virtual casing method provides the plasma current contribution to the normal component of the magnetic field strength on the plasma boundary by only evaluating a surface integral. For that, one only needs the tangential part of the magnetic field which is determined with a fixed-boundary VMEC calculation [22]. In addition, we target the length of the coils $L = \sum_j L_j$ with a scalar penalty functional $Q \equiv \varphi_2 + (L_t - L)^2$, where L_t is a user-specified target value for the sum of the compound coil length. Note that we choose a particularly simple target function with only two terms to focus on finding suitable coils, and plan to refine the target in future work.

Axisymmetric equilibria require a net toroidal plasma current to produce rotational transform and flux surfaces, inducing a significant vertical component in the targeted normal component of the external magnetic field on the plasma boundary D_n . To be able to obtain the typical tokamak toroidal field (TF) coils in the optimization procedure, one has to add poloidal field (PF) coils to cancel the vertical component of D_n . We started with four PF coils, where we only allowed the radius and the height z to vary.

Next we added 20 TF coils, with a large radius chosen to minimize coil ripple effects, as the geometry of the additional QA coils is our main interest; smaller and/or fewer TF coils may be used in future studies. These coils need not be optimized since only their total current is determined by the given equilibrium.

The perturbed axisymmetric equilibrium chosen for this study has four field periods and is stellarator symmetric. During optimization we initialized the additional QA coils as circular shapes located at the inboard side (not interlinked with the plasma boundary); the TF and PF coil geometries were held fixed during this optimization. Conventionally, stellarators employ so-called modular coil designs, like in Wendelstein 7-X or NCSX. However, to realize the unusual shape of our hybrid configuration, we found it more successful to choose QA coils that are not interlinked with the vacuum

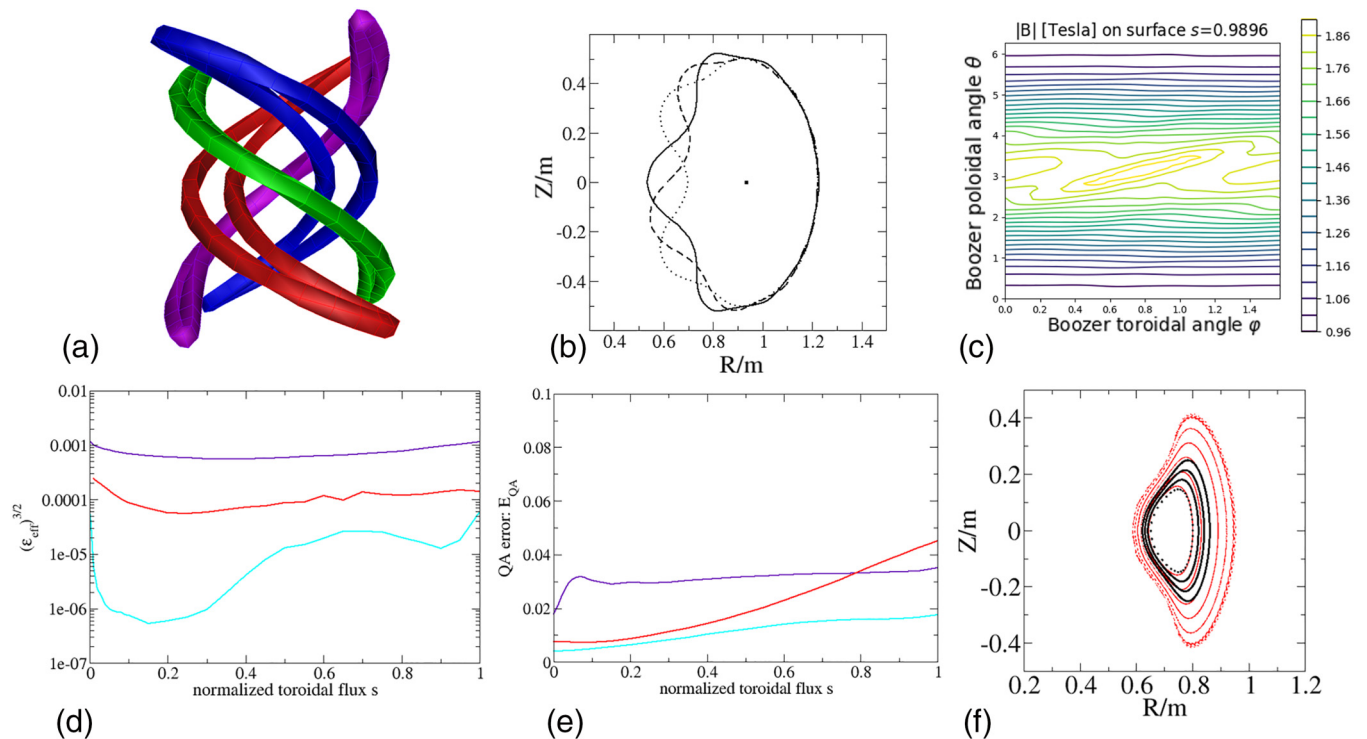


FIG. 4. Overview of results for the hybrid coil set: (a) The four identical QA (“banana”) coils—the only coils needed in addition to the standard tokamak coils. (b) The cross sections of the finite-beta plasma boundary with the original profiles evaluated with free-boundary VMEC [22] at three toroidal locations ($\varphi = 0^\circ, 22.5^\circ, 45^\circ$). (c) The contour lines of magnetic field strength with respect to Boozer angles, Ref. [11], near the plasma boundary for the original plasma profiles. (d) The effective ripple [23] to the power of 3/2 and (e) the quasisymmetric error, given by Eq. (2), (both evaluated based on VMEC outputs) vs the normalized toroidal flux s for three different profiles presented in this paper: the original profiles (cyan), the altered profiles from Ref. [14] (red), and the equilibrium with zero-beta and zero-net toroidal plasma current (purple). (e) Poincaré plots showing the flux surfaces in vacuum produced by solely TF and QA coils with the original coil currents in black and with altered QA coil current to increase volume in red at a single toroidal location, $\varphi = 0^\circ$ for clarity.

vessel, similar to saddle coils, except more elongated and carefully shaped.

To evaluate the quality of our quasisymmetry we use the quasisymmetric error defined as

$$E_{QA} = \left(\sqrt{\sum_{n \neq 0, m} B_{m,n}^2} \right) / B_{00}, \quad (2)$$

where the B_{mn} are the Fourier coefficients of the magnetic field in Boozer coordinates. Another measure used is the effective ripple ϵ_{eff} , which is a proxy for the neoclassical transport [23]. To aid comparison we present the effective ripple to the power 3/2.

Using free-boundary version of the ideal magnetohydrodynamic (MHD) equilibrium solver VMEC [22] with the magnetic field produced by our coils, we obtain the new plasma boundary and flux surfaces. To test if the quasisymmetry properties are maintained with the realization with the coils, we determine the quasisymmetric error from these VMEC equilibria.

Since it is not guaranteed that flux surfaces exist in vacuum [10], we evaluate the existence, shape, and volume of the flux surfaces by generating Poincaré plots based only on the coils’ magnetic field. We used the ROSE/ONSET suites [24]

to generate the Poincaré plots, and the plots of the quasisymmetric error and the effective ripple.

Results and Discussions. In addition to a set of standard tokamak coils (toroidal field (TF) and poloidal field (PF) coils [25]), we find that a single type of simple “QA coil” on the inboard side is sufficient to reproduce the perturbed QA equilibrium; see Fig. 4(a).

The equilibrium determined by the free-boundary VMEC code recreates the key feature of the boundary found from the analytic theory: the perturbation of the tokamak is dominantly located on the inboard side and the outboard side is mostly unaltered, see Fig. 4(b). The contours of constant magnetic field strength, plotted versus Boozer angles, look nearly straight everywhere except near the inboard midplane, and the Fourier harmonics also confirm the quasisymmetry feature, Fig. 4(c).

Both the effective ripple and the quasisymmetric error are measures of how well the stellarator is transport optimized, e.g., the effective ripple of CHS or TJ-II are as high as 30%–40% [26]. The effective ripple, Fig. 4(d), and the quasisymmetric errors, Fig. 4(e), are small when evaluated with the original profiles but also, surprisingly, with altered plasma profiles Fig. 3. For the altered plasma profiles we choose the one from Ref. [14] and the case of zero-net toroidal current and zero-plasma beta where the plasma beta β is the ratio of plasma pressure p and magnetic pressure $B^2/(2\mu_0)$. Even in this extreme case the effective ripple is below one

percent nearly everywhere which is comparable or even lower than in the largest transport-optimized stellarator Wendelstein 7-X or in the quasisymmetric design NCSX [26].

To further evaluate quasisymmetry quality, we calculated fast-particle losses of fusion-born alpha particles (3.5 MeV), initialized at half radius (e.g., quarter flux $s = 0.25$). Only 1.45% were lost after 0.2 seconds. This was evaluated with the SIMPLE code where 5000 particles were isotropically launched and followed, assuming no collisions [27,28]. The size of the machine was scaled to have the same minor radius of the QA reactor design ARIES-CS [29]. The observed confinement is better than most historic QA designs [8], though we emphasize that no QA optimization was performed (beyond the use of the approximately QA analytic solution) and also note that we use a magnetic field produced by coils, which typically have worse confinement due to field errors.

We find clear evidence of vacuum-flux surfaces in the Poincaré plots shown in Fig. 4(f). In such an experiment one has the freedom to control the volume of these flux surfaces by changing the QA coil current [see Fig. 4(f)] and also to control the added external rotational transform, reaching levels anywhere from zero to 0.3. This is in the range that has been shown in experiments to improve stability properties [4–7]. In these experiments it was found that an external rotational transform of around 0.1 to 0.15 can suppress disruptions.

A machine based on such a design would be a suitable candidate to study how 3D shaping affects plasma properties, such as stability, while approximately maintaining small neoclassical transport. In addition, one would be able to investigate if the plasma current can be ramped up starting from the vacuum-flux surfaces generated by the quasisymmetric coil currents. This “quasisymmetric startup” could be an alternative to ordinary Ohmic tokamak startup scenarios. Thus, there would be no need for a central solenoid, which is one of the most complex and expensive components of a conventional tokamak.

Since the QA coils are only on the inboard side, it might be possible to simply “upgrade” an existing tokamak by adding such coils. We note that inboard-type coils have indeed been realized in the past, e.g., at TEXTOR as part of a divertor concept [30]. However, the coils in this work will be larger than in TEXTOR and it might be necessary to remove the solenoid. In this case, our proposed alternative QA startup could be used.

For a major radius of around 1 m as we have presented here, the minimum coils-to-QA-plasma distance is 15 cm but only 6 cm for the distance between the QA coils and the

axisymmetric plasma boundary. If one scales this machine to a reactor size, e.g., of 1900 m³, this shortest coil-to-plasma distance increases to approximately 1.5 m. This distance for the QA operation is already (without including the distance into the optimization) relevant for a reactor-sized device, for which it is said that at least 1.5 m of space is needed for a breeding blanket and neutron shielding.

The aspect ratio of the QA stellarator depends on the chosen axisymmetric equilibrium which is perturbed with the analytic model outlined in Ref. [15,16]. This suggests that at any aspect ratio a hybrid design could be generated with the approach presented here as long as the QA coils can be made to fit in the center. Therefore our approach should permit designs comparable in compactness with previous tokamak-stellarator hybrids including the so-called “spherical stellarator” [1], while including the additional benefits described here, i.e., transport optimization, coil simplicity, etc.

The work presented here is an initial step in exploring our compact tokamak-hybrid concept. The equilibrium solutions so far considered represent a small part of the available space to explore. Indeed, any viable tokamak design can be considered a candidate for the application of our method (perhaps even axisymmetric equilibria that might not be considered for pure tokamak operation). This opens up a large optimization space for possible hybrid designs, over which quasisymmetry and other properties can be directly targeted, and further improved. MHD stability, divertor designs, and even microturbulence should also be investigated to see if the stellarator and tokamak strengths might also be favorably combined. These are just some of the possible activities to expand and refine our concept of the stellarator-tokamak hybrid.

Acknowledgments. We would like to thank Per Helander, Michael Drevlak, Robert Davies, and Brendan Shanahan for helpful discussions, Samuel Lazerson for the support with XGRID as well as helpful discussions, Caoxiang Zhu for help converting coil types within simsopt, Matt Landreman with general support with simsopt, Joachim Geiger for his support using free-boundary VMEC, and the simsopt development team. This work has been carried out within the framework of the EUROfusion Consortium, funded by the European Union via the Euratom Research and Training Programme (Grant Agreement No. 101052200—EUROfusion). Views and opinions expressed are however those of the author(s) only and do not necessarily reflect those of the European Union or the European Commission. Neither the European Union nor the European Commission can be held responsible for them.

[1] P. E. Moroz, Spherical stellarator configuration, *Phys. Rev. Lett.* **77**, 651 (1996).
 [2] P. E. Moroz, Extreme low aspect ratio stellarators, *Phys. Lett. A* **243**, 60 (1998).
 [3] K. Yamazaki and Y. Abe, TOKASTAR: a tokamak-stellarator hybrid with possible bean-shaped operation, Technical Report, Nagoya University, Japan, 1985.
 [4] W. V.-A. Team, Stabilization of the (2, 1) tearing mode and of the current disruption in the W VII-A stellarator, *Nucl. Fusion* **20**, 1093 (1980).

[5] M. Hirsch, J. Baldzuhn, C. Beidler, R. Brakel, R. Burhenn, A. Dinklage, H. Ehmler, M. Endler, V. Erckmann, Y. Feng, J. Geiger, L. Giannone, G. Grieger, P. Grigull, H.-J. Hartfuss, D. Hartmann, R. Jaenicke, R. Koenig, H. Laqua, H. Maassberg *et al.*, Major results from the stellarator Wendelstein 7-AS, *Plasma Phys. Control. Fusion* **50**, 053001 (2008).
 [6] M. D. Pandya, M. C. ArchMiller, M. R. Cianciosa, D. A. Ennis, J. D. Hanson, G. J. Hartwell, J. D. Hebert, J. L. Herfindal, S. F. Knowlton, X. Ma, S. Massidda, D. A. Maurer, N. A. Roberds, and P. J. Traverso, Low edge safety factor operation and passive

- disruption avoidance in current carrying plasmas by the addition of stellarator rotational transform, *Phys. Plasmas* **22**, 110702 (2015).
- [7] G. J. Hartwell, S. F. Knowlton, J. D. Hanson, D. A. Ennis, and D. A. Maurer, Design, construction, and operation of the compact toroidal hybrid, *Fusion Sci. Technol.* **72**, 76 (2017).
- [8] M. Landreman and E. Paul, Magnetic fields with precise quasisymmetry for plasma confinement, *Phys. Rev. Lett.* **128**, 035001 (2022).
- [9] J. Nührenberg, W. Lotz, and S. Gori, Quasi-axisymmetric tokamaks, edited by E. Sindoni, F. Troyon, & J. Vaclavic, in *Theory of Fusion Plasmas: Proceedings of the Joint Varenna-Lausanne International Workshop* (Editrice Compositori., Bologna, 1994), pp. 3–12.
- [10] P. Helander, Theory of plasma confinement in non-axisymmetric magnetic fields, *Rep. Prog. Phys.* **77**, 087001 (2014).
- [11] A. Boozer, Plasma equilibrium with rational magnetic-surfaces, *Phys. Fluids* **24**, 1999 (1981).
- [12] M. C. Zarnstorff, L. A. Berry, A. Brooks, E. Fredrickson, G.-Y. Fu, S. Hirshman, S. Hudson, L.-P. Ku, E. Lazarus, D. Mikkelsen, D. Monticello, G. H. Neilson, N. Pomphrey, A. Reiman, D. Spong, D. Strickler, A. Boozer, W. A. Cooper, R. Goldston, R. Hatcher *et al.*, Physics of the compact advanced stellarator NCSX, *Plasma Phys. Control. Fusion* **43**, A237 (2001).
- [13] M. Drevlak, F. Brochard, P. Helander, J. Kisslinger, M. Mikhailov, C. Nührenberg, J. Nührenberg, and Y. Turkin, ESTELL: A quasi-toroidally symmetric stellarator, *Contrib. Plasma Phys.* **53**, 459 (2013).
- [14] S. Henneberg, M. Drevlak, C. Nührenberg, C. Beidler, Y. Turkin, J. Loizu, and P. Helander, Properties of a new quasi-axisymmetric configuration, *Nucl. Fusion* **59**, 026014 (2019).
- [15] G. G. Plunk and P. Helander, Quasi-axisymmetric magnetic fields: weakly non-axisymmetric case in a vacuum, *J. Plasma Phys.* **84**, 905840205 (2018).
- [16] G. G. Plunk, Perturbing an axisymmetric magnetic equilibrium to obtain a quasi-axisymmetric stellarator, *J. Plasma Phys.* **86**, 905860409 (2020).
- [17] M. Landreman, Mapping the space of quasisymmetric stellarators using optimized near-axis expansion, *J. Plasma Phys.* **88**, 905880616 (2022).
- [18] S. A. Henneberg, S. R. Hudson, D. Pfefferlé, and P. Helander, Combined plasma-coil optimization algorithms, *J. Plasma Phys.* **87**, 905870226 (2021).
- [19] M. Landreman, B. Medasani, F. Wechsung, A. Giuliani, R. Jorge, and C. Zhu, Simsopt: A flexible framework for stellarator optimization, *J. Open Source Software* **6**, 3525 (2021).
- [20] B. Medasani, F. Wechsung, M. Landreman, E. Paul, A. Giuliani, R. Jorge, R. Gaur, C. Zhu, D. Staczak-Marikin, Z. Qudaringli, & tmqian, hiddenSymmetries/simsopt, Zenodo (2022), doi:10.5281/zenodo.7221578.
- [21] V. Shafranov and L. Zakharov, Use of the virtual-casing principle in calculating the containing magnetic field in toroidal plasma systems, *Nucl. Fusion* **12**, 599 (1972).
- [22] S. Hirshman and J. Whitson, Steepest-descent moment method for 3-dimensional magnetohydrodynamic equilibria, *Phys. Fluids* **26**, 3553 (1983).
- [23] V. Némov, S. Kasilov, W. Kernbichler, and M. Heyn, Evaluation of $1/\nu$ neoclassical transport in stellarators, *Phys. Plasmas* **6**, 4622 (1999).
- [24] M. Drevlak, C. Beidler, J. Geiger, P. Helander, and Y. Turkin, Optimisation of stellarator equilibria with rose, *Nucl. Fusion* **59**, 016010 (2019).
- [25] J. Wesson, *Tokamaks*, 3rd ed. (Oxford University Press, Oxford, UK, 2004).
- [26] C. Beidler, K. Allmaier, M. Isaev, S. Kasilov, W. Kernbichler, G. Leitold, H. Maassberg, D. Mikkelsen, S. Murakami, M. Schmidt, D. Spong, V. Tribaldos, and A. Wakasa, Benchmarking of the mono-energetic transport coefficients—results from the International Collaboration on Neoclassical Transport in Stellarators (ICNTS), *Nucl. Fusion* **51**, 076001 (2011).
- [27] C. G. Albert, S. V. Kasilov, and W. Kernbichler, Accelerated methods for direct computation of fusion alpha particle losses within, stellarator optimization, *J. Plasma Phys.* **86**, 815860201 (2020).
- [28] C. G. Albert, S. V. Kasilov, and W. Kernbichler, Symplectic integration with non-canonical quadrature for guiding-center orbits in magnetic confinement devices, *J. Comput. Phys.* **403**, 109065 (2020).
- [29] F. Najmabadi, A. R. Raffray, and The ARIES-CS Team, The ARIES-CS compact stellarator fusion power plant, *Fusion Sci. Technol.* **54**, 655 (2008).
- [30] O. Neubauer, G. Czymek, B. Giesen, P. W. Hüttemann, M. Sauer, W. Schalt, and J. Schruoff, Design features of the tokamak textor, *Fusion Sci. Technol.* **47**, 76 (2005).